TRENDS IN SCIENCES 2025; 22(10): 10383
https://doi.org/10.48048/tis.2025.10383
REVIEW ARTICLE

Advances in Optical Fiber Sensing Using Gold/Silver Nanocomposites: A Review

Siti Azimatul Luthfiyyah[1], Sunaryono[1], Hazri Bakhtiar[2], Arif Hidayat[1] and Nurul Hidayat[1,3,4,*]

[1]Department of Physics, Faculty of Mathematics and Natural Sciences, Universitas Negeri Malang, Malang 65145, Indonesia
[2]Laser Center, Ibnu Sina Institute for Scientific and Industrial Research, Universiti Teknologi Malaysia, Skudai 81310, Malaysia
[3]Center for Instrumentation and Sensing Technology, Universitas Negeri Malang, Malang 65145, Indonesia
[4]Center for Science and Engineering, Universitas Negeri Malang, Malang 65145, Indonesia

([*]Corresponding author's e-mail: nurul.hidayat.fmipa@um.ac.id)

Received: 16 April 2025, Revised: 24 May 2025, Accepted: 30 June 2025, Published: 20 July 2025

Abstract

The past 20 years have witnessed a marked increase in research focused on optical fiber sensors for their potential to detect changes due to physical and chemical properties. Various modifications on optical fibers have been explored to improve their sensing performance and application-specific suitability. One such approach involves the coating of optical fibers with plasmonic nanomaterials, enabling the activation of Localized Surface Plasmon Resonance (LSPR) effect. Among these, gold/silver nanocomposites (Au/Ag NCs) demonstrate strong LSPR effect that can enhance the sensitivity of optical fiber sensors. Diverse functionalization techniques have been developed to integrate these plasmonic nanomaterials effectively, while the structural configuration of the optical fiber is equally critical for attaining optimal sensing performance. This review highlights the role of Au/Ag NCs in advancing optical fiber capabilities, explores relevant fiber structures, examines the limitations and challenges, and discusses potential applications in healthcare, industry, and environmental monitoring. Finally, future research directions are proposed to guide further innovation in this rapidly evolving field.

Keywords: Optical fiber, Gold/silver nanocomposite, Plasmonic functionalization, Sensing application

Glossary

AgNPs	Silver Nanoparticles
APMES	(3-Aminopropyl)ethoxysilane
APTES	(3-Aminopropyl)triethoxysilane
AuNPs	Gold Nanoparticles
Au/Ag NCs	Gold/Silver Nanocomposites
CAGR	Compound Annual Growth Rate
COVID-19	Corona Virus Disease 2019
FBG	Fiber Bragg Grating
FPI	Fabry-Perot Interferometer
GO	Graphene Oxide
HCF	Hollow-Core Fiber
HR-TEM	High Resolution-Transmission Electron Microscopy
LCC	Liquid Crystal Cladding
LSPR	Localized Surface Plasmon Resonance

MMF	Multi Mode Fiber
MMI	Multi-Modal Interference
MPTMS	(3-Mercaptopropyl)trimethoxysilane
MZI	Mach Zehnder Interferometer
NCF	No-Core Fiber
NCs	Nanocomposites
PDMS	Polydimethylsiloxane
PS	Peanut Structure
PVA	Polyvinyl Alcohol
RH	Relative Humidity
SAM	Self Assembly Monolayer
SDGs	Sustainable Development Goals
SARS-CoV-2	Severe Acute Respiratory Syndrome Coronavirus 2
SERS	Surface-Enhanced Raman Scattering
SMF	Single Mode Fiber
SPR	Surface Plasmon Resonance
TCF	Thin Core Fiber
TFBG	Tilted Fiber Bragg Grating
TCF	Thin-Core Fiber
TOF	Tapered Optical Fiber
UV-Vis	Ultraviolet-Visible
XRD	X-Ray Diffraction

Introduction

Optical fiber sensors apply optical methods to measure various physical and chemical properties in modern technological developments. Recent studies have examined the potential of optical fibers as sensors, as documented by many publications reporting their applications in chemical sensing [1-4], gas detection [5,6], humidity monitoring [7,8], biosensing [9,10], salinity measurement [11,12], and many other fields. The use of nanoplasmonic materials play critical role in the advancements of optical fiber sensing technology. Recent advances have also showed how Au/Ag NCs improved optical fiber sensing sensitivity compared to conventional sensors [11]. The integration of plasmonic Au/Ag nanostructures enabled detection limits down to picomolar concentrations for biosensing applications [13]. Moreover, optical fiber sensors have a relatively long service life, typically at least ten years, as demonstrated in previous study [14]. Based on the Verified Market Research report, the global optical fiber sensor market was valued at $ 4.506 billion in 2024 and is forecasted to grow $8.56 billion by 2031 having a compound annual growth rate (CAGR) of 10.80%. Nanocomposite-enhanced optical fiber sensors represent the fastest-growing segment, accounting for approximately 25% of this market [8]. Cost-benefit analyses show that these advanced sensors reduce operational costs by 30% - 40% in industrial monitoring applications due to their durability and precision [9]. Furthermore, the healthcare biosensing market utilizing Au/Ag NCs sensors is expected to reach $1.2 billion by 2028, driven by point-of-care diagnostics demand [10]. The optical fiber sensing technology development is in line with the goals of the United Nations, including building resilient infrastructure (SDG 9), where optical fiber sensors are applicable in the industrial fields [15]. In addition, the potential use of optical fiber sensors in the fields of healthcare, such as in biomedical diagnostics and patient monitoring [16], as well as in in environmental monitoring, for example water quality analysis and air pollution detection [17]. These applications are well aligned with SDG 3 (good health and well-being), SDG 6 (clean water and sanitation), SDG 13 (climate action), and SDG 14 (life below water). Thus, optical fiber sensing technology contributes significantly to multiple SDGs. In the context of green and sustainable development, optical

fiber sensors provide to real-time [18], energy-efficient [19], and low-carbon monitoring systems [20]. Their compact size, resistance to electromagnetic interference, and long-term stability make them ideal for integration into green technologies, such as renewable energy systems [21], smart cities [22], and ecological conservation efforts [23]. For example, they can be deployed in smart irrigation systems to optimize water usage in agriculture [24] or in offshore platforms to detect marine pollutants [25], thereby supporting environmental sustainability. Through these diverse applications, optical fiber sensing technology not only enhances technical performance across sectors but also fosters a greener, more sustainable future in alignment with global environmental and development goals.

The growing demand for high transmission speed and data accuracy has driven researchers to develop optical fiber sensors with improved capabilities. One such development techniques involves modifying the optical fiber structure. For instance, Ding *et al*. [7] utilized single mode fiber (SMF) forming a balloon-like interferometer for humidity sensor. Tang *et al*. [2] employed no-core fiber (NCF) connected to an SMF to detect structural steel corrosion. Besides structural modification, coating optical fiber with plasmonic nanomaterials is also effective to enhance the sensing operation. For this purpose, Kong *et al*. [26] reported that the plasmonic nanomaterials significantly increased the tumor cell sensing sensitivity up to 5 times higher than that of uncoated fiber. Various nanostructures have since been applied in optical fiber-based sensors, including gold nanoparticles (AuNPs) for refractive index sensing [27], Au@Ag nanohybrid structures for biosensors [9], Ag@Fe_3O_4 NCs for H_2S detection [28], Ag/Cu NCs for effective petroleum sensing [29], and Au-assisted SiO_2-TiO_2 NCs for pH sensor [30]. These examples highlight that Au and Ag nanostructures are among the most applied materials in optical fiber sensors. This results from the fact that AuNPs and AgNPs exhibit unique LSPR peaks [31], and their combination can expand the wavelength range especially when applied in optical fiber sensors [32]. Therefore, the development of Au/Ag NCs offers a promising strategy for enhanced optical fiber sensing performance. Numerous studies have exclusively investigated Au/Ag NCs into various optical fiber sensing applications, such as for quick sensing of C-reactive protein [9], vitamin A [33], cyanide in water [34], refractive index [35], and many more.

Plasmonic materials, notably Au and Ag, are capable of generating optical phenomena - including localized and surface plasmon resonances (LSPR and SPR) - which contribute to enhancing the sensitivity of optical fiber sensors. LSPR occurs in plasmonic nanoparticles having size less than 100 nm, where incident light excites collective electron oscillations that couple with confined light waves around the nanostructures [36]. This interaction significantly enhances the local electromagnetic field near the nanoparticle surface, which in turn increases the sensitivity to the surrounding refractive index alteration [37]. While LSPR is typically associated with plasmonic nanoparticles, SPR occurs in continuous plasmonic films. SPR takes place when the momentum of the incident electromagnetic light wave matches that of the surface plasmon, leading to resonance [38].

Many other reviews have been published especially in optical fiber sensors. For instance, Mahmud *et al*. [39] reviewed SPR-activated optical fiber for biosensing applications. Zhang *et al*. [40] discussed various approaches for heavy metal ion concentration measurements using optical fiber sensors, including plasmonic-based approach. However, their review provided only the general overview of the role plasmonic materials. In other words, there remains a lack of exclusive reviews specifically focusing on the role of Au/Ag NCs in enhancing the performance of optical fiber sensors. To address this gap, this review offers a comprehensive overview of the impact of Au/Ag NCs for improved optical fiber sensors. It also discusses various optical fiber structures and nanocomposite coating techniques. Furthermore, the review explores potential applications of Au/Ag NCs-coated optical fiber sensors, outlines current limitations and challenges, and suggests directions for future research.

Gold/silver nanocomposites

Au/Ag NCs are composite materials composed of AuNPs and AgNPs with sizes less than 100 nm. Au/Ag NCs are classified as noble metal nanocomposites that have superior biocompatibility [41], good photoluminescence [42,43], excellent photostability, and versatile for functionalization [44]. Therefore,

Au/Ag NCs can be applied in various fields, including in optical fiber sensing technology. Au/Ag NCs have been widely studied for various sensor applications, including biosensors for quick observation of C-reactive protein [9], vitamin A [33] and B1 [45], cyanide in water [34], and refractive index [35,46,47].

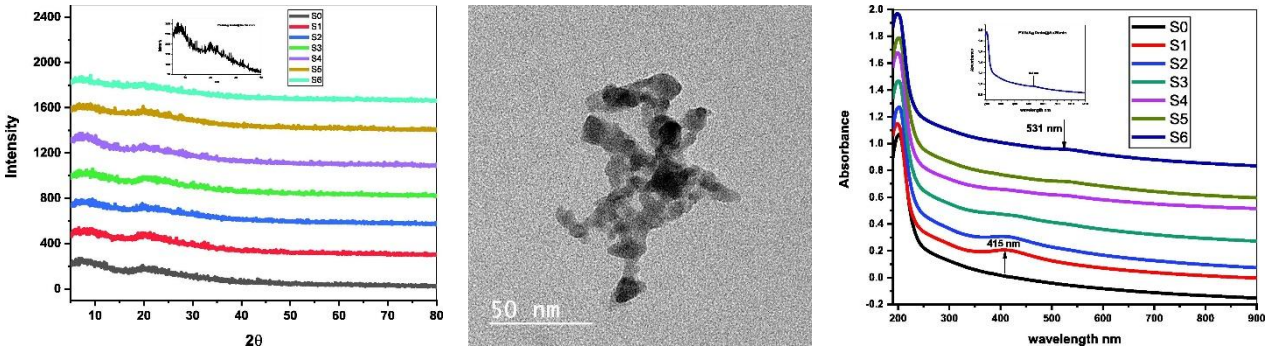

(a) (b) (c)

Figure 1 (a) XRD profiles, (b) HR-TEM photograph, and (c) UV-Vis spectra of Ag/Au NCs produced by Nd:YAG laser ablation method [48].

There are 2 main approaches to synthesize Au/Ag NCs: The top-down and bottom-up routes. In the top-down approach, Au/Ag NCs are produced by breaking down bulk materials into nanoscale structures. An example of a top-down approach is pulsed laser ablation [48]. In contrast, the bottom-up approach involves the formation of Au/Ag NCs through chemical reactions from molecular precursors. Ultrasonic-assisted growth and chemical reduction, as demonstrated by Phuong *et al*. [9]; Bi *et al*. [49], are representative bottom-up routes. Bi *et al*. [48] described that Au/Ag NCs synthesized in polyvinyl alcohol (PVA) by Nd:YAG laser ablation method had X-ray diffraction (XRD) peaks with decreasing intensity along with increasing AgNPs content and varying ablation times (**Figure 1(a)**). Morphological analysis via high resolution-transmission electron microscopy (HR-TEM) revealed that the shape of Au/Ag NCs were spherical with some agglomeration and exhibited core-shell structures with size ranges between 7 and 29 nm (**Figure 1(b)**) [48]. Furthermore, an increase in the absorption peak was observed by ultraviolet-visible (UV-Vis) spectroscopy with longer ablation times (**Figure 1(c)**), indicating enhanced complexation between the metal nanoparticles and the polymer matrix [48].

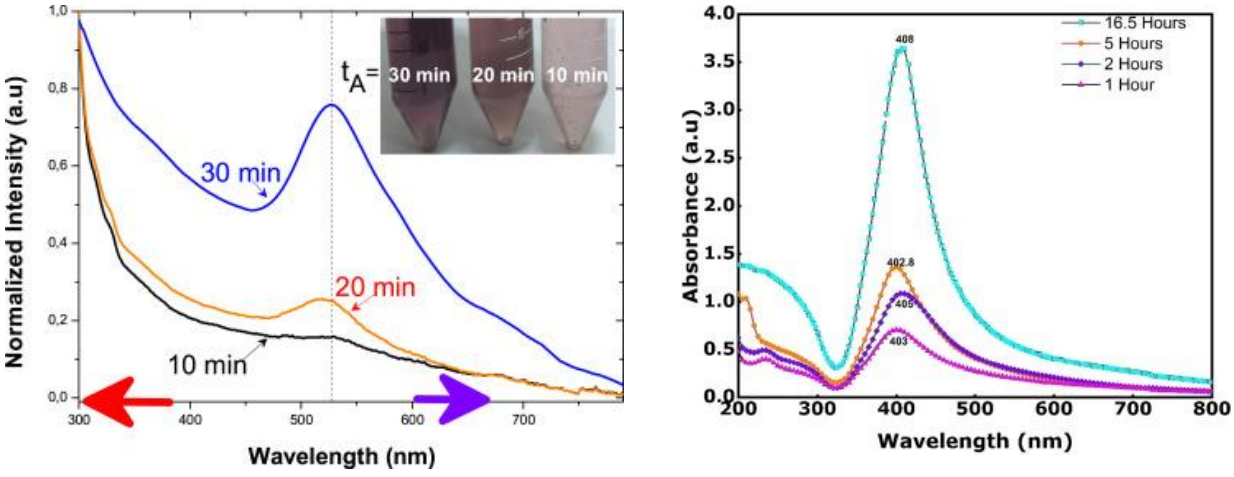

(a) (b)

Figure 2 Plasmonic characteristics of (a) AuNPs [50] and (b) AgNPs [51].

The synthesis duration of Au/Ag NCs significantly influences their LSPR characteristics. One method of making Au/Ag NCs is by mixing Au and Ag nanocolloidal solutions. In this sense, temporal changes in the LSPR peak could be observed during the individual synthesis processes of AuNPs and AgNPs. A previous study [50] reported that AuNPs synthesized by the laser ablation method, with ablation times ranging from 10 to 30 min, exhibited a red shift of about 7 nm in the LSPR peak (**Figure 2(a)**). Similarly, another study investigating the effect of synthesis time on AgNPs reported time-dependent shifts in the LSPR peak position (**Figure 2(b)**) [51]. Furthermore, the HR-TEM image of Au@Ag nanostructures is shown in **Figure 3(a)**, showing core-shell structure. The LSPR profiles of AuNPs and Au@Ag NCs are given in **Figure 3(b)**, indicating the coexistence of the plasmonic peak of AuNPs and AgNPs.

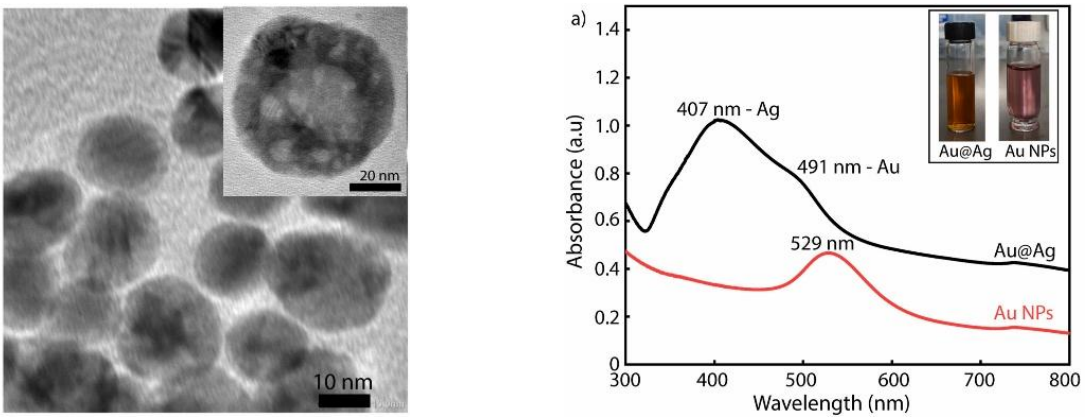

(a) (b)

Figure 3 (a) Morphological and (b) optical properties of Au@Ag NPs synthesized using bottom-up approach [9].

Table 1 presents a comparative summary of Au/Ag NCs synthesized using different methods, focusing on their particle sizes and corresponding LSPR peak positions (λ). From **Table 1**, it is obvious that different synthesis techniques yield in different particle sizes and LSPR characteristics. Nd:YAG laser ablation produced PVA-stabilized Au/Ag NCs with a size range of 7 - 29 nm. This relatively wide size distribution suggested some degree of agglomeration, which might arise from the laser ablation process in a PVA matrix. The LSPR peaks for AgNPs and AuNPs were occurred at 412 and 531 nm, respectively [48]. Furthermore, the ultrasonic-assisted growth and chemical reduction method yielded Au@Ag core - shell nanostructures with averaging 20 nm in diameter, as depicted also in **Figure 3(a)** [9]. As shown in **Table 1** and **Figure 3(b)**, this method produced multiple LSPR peaks corresponding to AgNPs (407 nm), AuNPs (529 nm), and Au@Ag core-shell structures (491 nm). In another study, simultaneous reduction of gold and silver ions using produced Au/Ag NCs with a larger particle size of approximately 55 nm [49]. The LSPR peaks were located at 417 nm for AgNPs and 525 nm for AuNPs. In addition, the wet chemical synthesis Au@Ag NCs with a particle size of 24 nm and LSPR peaks at 498 nm (AuNPs) and 404 nm (AgNPs) [52].

Table 1 Characteristics of Au/Ag NCs produced by different synthesis methods.

Materials	Synthesis Method	Diameter (nm)	λ (nm)	Ref.
PVA-Au/Ag NCs	Nd:YAG laser ablation	7 - 29	AgNPs = 412 AuNPs = 531	[48]
Au@Ag nanostructures	Ultrasonic-assisted growth and chemical reduction	20	AuNPs = 529 Au@Ag NP = 491 AgNPs = 407	[9]

Materials	Synthesis Method	Diameter (nm)	λ (nm)	Ref.
Au/Ag nanostructures	Simultaneous reduction	55	AuNPs = 525 AgNPs = 417	[49]
Au@Ag nanostructures	Wet chemical synthesis	24	AuNPs = 498 AgNPs = 404	[52]
Au/Ag NCs	Wet chemical synthesis	21	-	[53]

Optical fiber structures for sensing application

Optical fiber sensors represent a significant innovation in measurement technology based on optical methods. Optical fibers offer multiple benefits when used as sensors, such as resistance to corrosion, immunity to electromagnetic interference, combined sensing and signal transmission capabilities, and suitability for operation in harsh environments [54]. Various types of optical fibers have been studied and modified for sensor applications across diverse fields, as summarized in **Table 2**. These modifications aim to optimize sensor performance for specific detection requirements.

Table 2 Optical fiber structures and their sensing applications.

Sensing Application	Optical Fiber Structure	Sensitivity	Detection Range	Coating Material	Ref.
Humidity Sensor	SMF-PS-MMF-PS-SMF	0.663 nm/% RH	50% - 80%	Gelatin	[55]
	SMF-structure enlarged waist-SMF with lining material-structure enlarged waist-SMF	0.193 dB/% RH	25% - 80%	GO/PVA	[56]
	SMF-TFBG-SMF	0.129 dB/% RH	10% - 80%	GO	[57]
Temperature Sensor	SMF-HCF-SMF	−4.08658 nm/°C	20 - 48 °C	PDMS	[58]
	FPI_s (SMF-UV-SMF) flow into FPI_{r1}	10 nm/°C	-	-	[59]
	FPI_s (SMF-UV-SMF) flow into FPI_{r2}	15 nm/°C			
	FPI_s (SMF-UV-SMF) flow into FPI_{r3}	22 nm/°C			
	MZI (TCF-NCF-TCF)	130 pm/°C	50 - 80 °C	PDMS	[60]
Ethanol Gas Sensor	SMF-MMF-SMF	3.85 pm/ppm	0 - 250 ppm	$ZnSnO_3/TiO_2$	[61]

Optical fiber sensors can be designed with various structural configurations to suit specific application requirements. Each structure typically consists of a combination of several types of optical fibers. For example, in humidity sensors, the optical fiber structure generally uses the Single Mode Fiber (SMF) type, while the sensing region - the part that directly interacts with the target - may utilize different type of optical fiber tailored for enhanced sensitivity. Various structures were investigated to produce the best sensor performance. SMFs were widely used by previous researchers because they can measure small changes in the phase of light propagating through the sensing region [62]. In addition, SMFs can transmit signals at

higher speeds compared to that of Multimode Fibers (MMFs), as it avoids modal dispersion and modal noise [63]. Dispersion occurs in MMFs because different propagation modes travel at varying speeds, leading to modal dispersion [64]. Modal noise is also associated with MMF and does not occur in SMF, where the optical power is distributed unevenly among a number of modes resulting in speckle patterns on the detector. SMF has a very small core diameter (5 - 10 μm) which serves to limit the transmission to a single mode, but incorporating light into SMF also requires tighter tolerances compared to optical fibers that have a larger core diameter [63].

.

Based on **Table 2**, MMFs are also used in several optical fiber sensor applications, such as humidity sensors [55] and ethanol gas detection sensors [61]. MMFs have a larger core compared to the wavelength of light, so that the optical phenomena that occur can be described with a geometric optics approach [65]. In this approach, light is treated as a collection of rays traveling in straight lines within the fiber. When these rays encounter interfaces separating media of differing refractive indices, they undergo reflection and/or refraction, as illustrated in **Figure 4**.

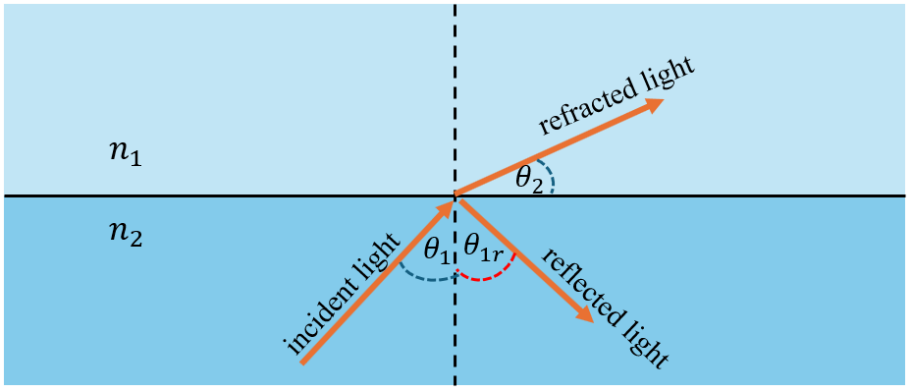

Figure 4 Illustration of light refraction and reflection.

The reflection and refraction of light that occurs in different media can be explained by the law of geometric optics which states that

$$\theta_{1r} = \theta_1 \quad (1)$$

and

$$n_1 \sin\theta_1 = n_2 \sin\theta_2 \quad (2)$$

where θ_{1r} denotes the reflection angle, θ_1 represents the incidence angle, θ_2 indicates the refraction angle, n_1 is the refractive index of medium 1, and n_2 that of medium 2.

Based on Eq. (2), if $n_1 > n_2$, then $\theta_2 = \pi/2$ radians, and this occurs when $\theta_1 = \sin^{-1} n_2/n_1$. As θ_1 increases beyond a certain critical value, refraction no longer occurs, causing the incoming light to be entirely reflected within the medium - a process termed total internal reflection [65]. In optical fibers, this effect takes place at the interface between the cladding and the core.

As depicted in **Figure 5**, total internal reflection can be described using Snell's Law. When the incident angle surpasses the critical threshold, the light does not transmit into the cladding but remains fully reflected inside the core. It has a consequence that

$$\theta_0 < \theta_0^{max} = \sin^{-1} \frac{\sqrt{n_1^2 - n_2^2}}{n_0} \quad (3)$$

where n_0 is the refractive index of air and θ_0 is the incidence angle. Due to total internal reflection, light is retained within the core and can effectively transmit along the entire optical fiber [65]. A larger core diameter affects both the attenuation and dispersion of light propagating through the fiber. In MMFs, multiple modes propagate simultaneously, each experiencing different attenuation and dispersion characteristics due

to their distinct reflection patterns within the core [66]. The difference in attenuation and dispersion of the beam light passing through the MMF will impact the signal captured by the detector.

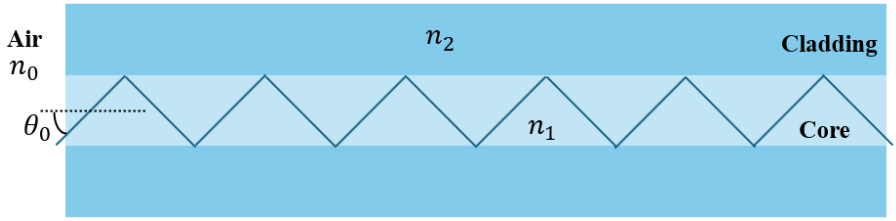

Figure 5 Illustration of total internal reflection in optical fiber.

Some previous studies have used MMFs as sensor structures that interact with the target, for example in the applications of humidity [55] and ethanol gas [61] sensors. When light beams from different types of optical fibers enter the MMF core, some rays may also enter the cladding. The light that couples into the MMF core can excite higher-order core modes. This change is used as a basis to determine the sensitivity of optical fiber sensors in detecting an analyte. The interference intensity in optical fibers *I*, can be represented as [55]:

$$I = \sum_{i=1}^{n} I_{core}^{i} + \sum_{j=1}^{m} I_{clad}^{j} + 2\sum_{i=1}^{n}\sum_{j=1}^{m}\sqrt{I_{clad}^{j} I_{core}^{i}}\cos\left(2\pi\left(\Delta n_{eff}^{i,j}\right)\frac{L}{\lambda}\right) \quad (4)$$

where i and j respectively represents the core and cladding. $\Delta n_{eff}^{i,j}$, λ, and L indicate the core-cladding refractive index difference, the light wavelength, and the length of the optical fiber, respectively.

No-Core Fiber (NCF) is another type of optical fiber that is also widely applied as sensors. It is an optical fiber without a defined core that enables the guided light to interact directly with the external medium or analyte. When a light beam from another type of optical fiber enters the NCF, multiple high-order modes are excited. these modes interfere along the propagation path, forming self-image effect [60,67]. A portion of the propagated light in the NCF interacts with the surrounding analyte, while the remainder continues to transmit through the fiber. This results in different optical paths for the 2 light beams. The difference in optical path length introduces a phase difference between them, which can be quantified using Eq. (5) [33].

$$\phi = \frac{2\pi\Delta n_{eff} L}{\lambda} \quad (5)$$

where Δn_{eff} can be represented through Eq. (6).

$$\Delta n_{eff} = n_{core} - n_{cladding+additiona\ layer}^{effect} \quad (6)$$

Accordingly, the interference intensity in the NCF is formulated in Eq. (4), while the self-imaging effect, driven by the superposition of excited high-order modes, is represented by Razali *et al.* [67]:

$$E(x, y, 0) = \sum_m c_m F_m(x, y) \quad (7)$$

where $E(x, y, 0)$ is the electric field profile originating from the previous optical fiber (e.g. SMF). While F_m is the spatial field and c_m is the excitation coefficient. The subscript *m* indicates the of the order of field eigenmode. c_m is defined by Eq. (8) [67].

$$c_m = \frac{\int_0^{\infty}\int_0^{\infty} E(x,y,0)F_m(x,y)dxdy}{\int_0^{\infty}\int_0^{\infty} F_m(x,y)F_m(x,y)dxdy} \quad (8)$$

The electric field profile evolving along the NCF is expressed by Razali *et al.* [67]:

$$E(x, y, z) = \sum_{m=1}^{N} c_m F_m(x, y)\exp(j\beta_m z) \quad (9)$$

where β_m corresponds to the longitudinal propagation constant associated with the m^{th}-order mode.

In addition, there are also several other types that are used and modified to obtain maximum sensing

performance, such as Fiber Bragg Grating (FBG) and Tilted Fiber Bragg Grating (TFBG). TFBG is characterized by a periodic grating structure inscribed at a specific tilt angle relative to the optical fiber axis [68]. This angular tilt provides distinctive functions such as coupling, dispersion, and light deflection [69]. Furthermore, the strong core-cladding mode coupling one of the prominent characteristics of TFBG [70]. The high sensitivity and good sensing ability [71], for example in chemical and biological sensing, make TFBGs widely used as sensors in the chemical and biological fields. TFBG is a modified form of FBG that is commonly used for strain sensing. FBGs possess excellent multiplexing capabilities and immunity to electromagnetic interference, which has led to their widespread use in measuring temperature and strain across various engineering applications [72]. FBG is characterized by modulation of periodic refractive index modulation in the core [73]. When broadband light propagates in the fiber grating, the Bragg wavelength is reflected and defined by Eq. (10) [74].

$$\lambda_B = 2n_{eff}\Lambda \quad (10)$$

where λ_B, n_{eff}, and Λ represent respectively the Bragg wavelength, the core's refractive index, and the periodic spacing of the grating.

When an FBG is exposed to external influences such as temperature, pressure, strain, or vibration, shifts in the Bragg wavelength occur, accompanied by variations in the core's refractive index and periodic spacing [72]. The Bragg wavelength shift can be represented by Eq. (11) [75].

$$\Delta\lambda_B = \lambda_B(1 - Pe)\Delta\varepsilon + (\alpha + \zeta)\Delta T \quad (11)$$

where $Pe, \Delta\varepsilon, \alpha,$ $\zeta,$ and ΔT indicate the electrooptic constant, strain, thermal expansion coefficient, thermo-optic coefficient, and temperature change, respectively.

Au/Ag NCs coating on optical fibers

Plasmonic materials have been extensively employed in optical fiber sensors to improve sensing sensitivity. Numerous studies have documented the application of Au/Ag NCs coatings on different optical fiber sensor types. For example, they were coated on optical fiber for C-reactive protein rapid detection in biosensing field [9]. Huang *et al*. [13] and Phuong *et al*. [34] also coated Au@Ag-Pt NCs and Au@Ag on optical fibers as copper (II) ion and cyanide detections. Various methods have been used to coat Au/Ag NCs on optical fiber sensors. These methods include self-assembly monolayer (SAM) [36], electroless plating [76], and photochemical deposition [77].

SAM involves the use of coupling agents with specific terminal groups to modify the optical fiber surface, enabling the attachment of nanoparticles, as illustrated in **Figure 6** [36]. Some materials coated on optical fibers using this approach include Au nanospheres [36], AuNPs capped with palladium [78], and chitosan-coated AuNPs [79]. Before the coating takes place, activation of the optical fiber surface is carried out. Hidayat *et al.* [36] in their research cleaned the optical fiber to be activated using methanol by soaking. After cleaning, the optical fiber was soaked using NaOH for OH groups activation on the fiber surface. In addition to using NaOH, other studies have also used a piranha solution consisting of hydrogen peroxide and sulfuric acid for the activation of hydroxyl groups [78]. Prior to the subsequent step, the optical fiber was initially dried and subsequently immersed in a 1% MPTMS solution prepared in ethanol [36] with the aim of activating thiol (-SH) functionalization or nanoparticle coupling agents. In activating coupling agents, some researchers also employed ethanol containing 1% APTES [79] or APMES (20 µL) contained in isopropyl alcohol (4 mL) [78]. After the coupling agent is activated, the optical fiber is immersed into the colloidal nanoparticles to be immobilized for several days. The duration of immersion starting from the surface activation process of the optical fiber until the activation of the coupling agent can be varied to produce maximum final results.

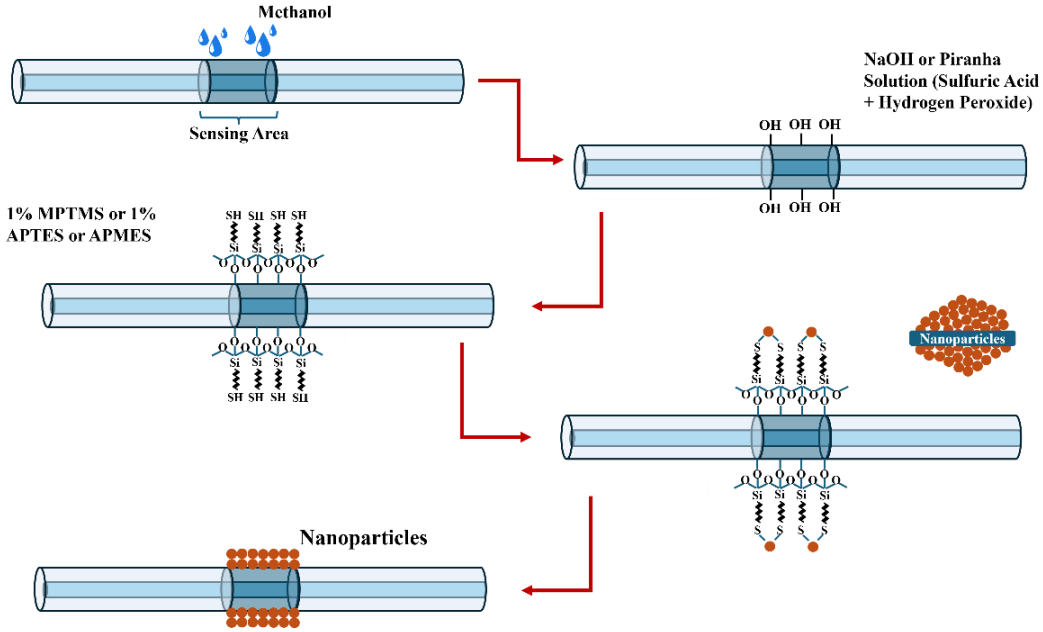

Figure 6 Illustration of nanoparticles coating using SAM method.

Electroless plating is another coating method commonly used optical fiber surface functionalization purposes. This method is widely adopted due to its ease of implementation, low-cost equipment requirements, and flexibility in application [80]. This nanoparticle coating technique operates without electrical power, relying instead on the chemical reduction of metal ions using reducing agents, for example, hydrazine, formaldehyde, hydroxylamine, and glucose [76]. This method can be applied to conductive or non-conductive objects (such as optical fibers). It is able to produce discontinuous layers that enables evanescent waves to interact with the outer layer and the analyte [76]. This method relies on electron kinetics during the coating process, in which the slow transfer of electron transfer from the reducing agent to metal ions limits the reduction of other ions. The use of a catalyst on the surface of substrates like optical fibers during the coating process serves to increase the reduction rate of metal ions, thereby enabling the formation and growth of the coating [76]. For instance, in the study reported by Loyez *et al.* [80], reducing agents to convert Au^{3+} to Au^{0} through electron transfer process producing Au thin film deposition. Illustration of the electroless coating method applied in a sandwich assay for thrombin detection is shown in **Figure 7.**

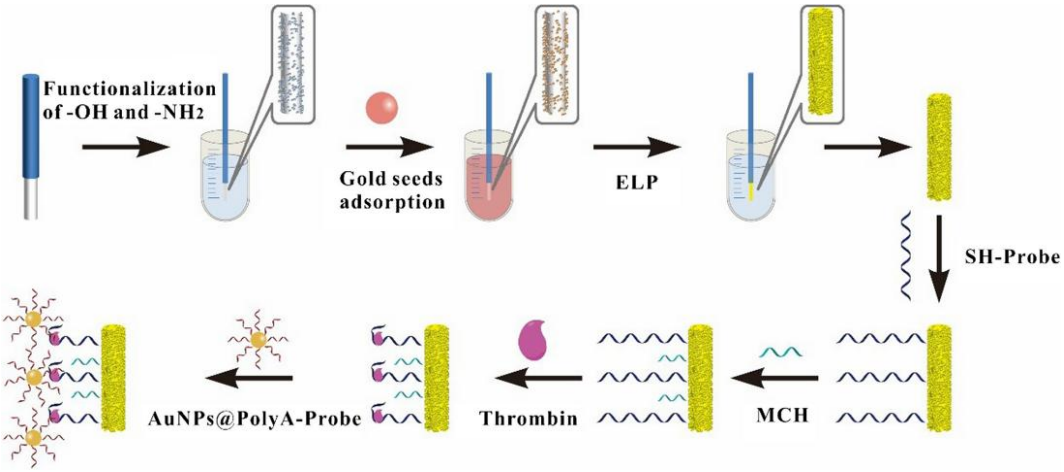

Figure 7 Illustration of the electroless plating method on optical fiber and its application in a sandwich assay for thrombin detection [81].

Furthermore, photochemical deposition can be applied as a method of nanoparticles coating or thin films formation on optical fibers. This technique controls the photosensitive properties and SPR response ability of certain elements such as Au and Ag to synthesize nanoparticles with customized size and shape [82]. Photochemical deposition enables the nanoparticles coating on the optical fiber tip and core [77]. It has several advantages, such as simple, low cost, controllable during coating, selective deposition site, and fast deposition process [83]. However, it is limited by the range of materials that can be effectively deposited. Materials commonly used with this method include AgNPs [82] and AuNPs [77].

As illustrated in **Figure 8**, a semiconductor laser is used during the deposition process, and the form of nanoparticles to be deposited should be in colloidal form. However, samples in colloidal form have some drawbacks, especially when applied to Surface-Enhanced Raman Spectroscopy (SERS) substrates, namely poor stability in suspension [82]. An investigation was conducted using a semiconductor laser emitting at 638 nm with a fiber tip output power of 35 mW to achieve the AgNPs deposition on the ends of the fibers [83]. Another study utilized a semiconductor laser with a working wavelength of 635 nm and power of 15 mW [77]. In this technique, the optical fiber intended for deposition must first be cleaved to produce a flat end face [83]. Subsequently, the fiber tip is immersed in the reaction solution containing Na_3Ct and gNO_3 [83]. Following this, laser light is transmitted into the reaction solution via the fiber core. Thus the laser irradiation will trigger the gradual formation and deposition of nanoparticles [83]. The deposition of nanoparticles can be controlled based on the laser irradiation time

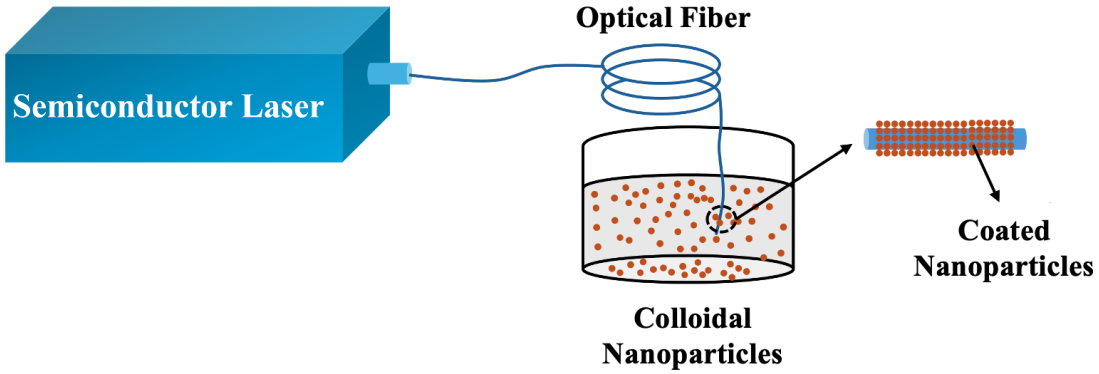

Figure 8 Illustration of nanoparticles coating by photochemical deposition method.

Functionalization of optical fiber sensors is not limited to surface coating; other methods involve incorporating additional materials during fiber fabrication, which can influence sensor performance. This method is 3D Printing [84,85]. Based on previous research [65], optical fibers could be printed using a 3D printer and begin by feeding the prepared resin into the resin barrel. The printing process commences with UV light emitted from the printer's lower section, which cures the first layer of resin onto the printing platform. After each layer has dried, the printing plate moves up slightly, according to the thickness of the layer. The process of multimaterial printing on optical fibers entails first depositing one material, then temporarily halting the operation to change the barrel to a different material and subsequently completing the printing of the remaining sections [65]. The illustration of this method is shown in **Figure 9**.

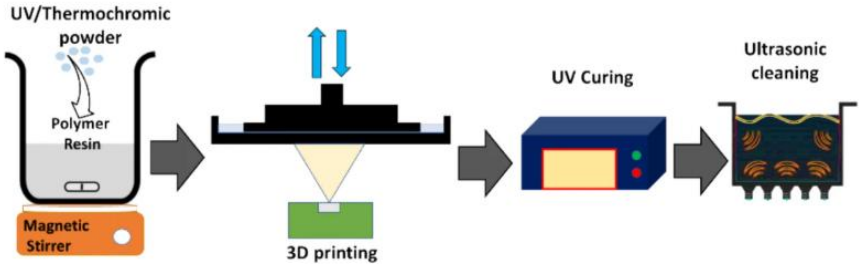

Figure 9 Illustration of 3D printing in optical fiber sensors [65].

Various approaches of functionalization of plasmonic materials on optical fibers have been discussed. These affect the thickness of the functionalized plasmonic material layer. The performance of optical fiber sensors is influenced by the thickness of the plasmonic material layer. The SAM technique offers potential for precisely controlling this layer's thickness on optical fibers. However, if the coating is carried out when manufacturing optical fibers, then the 3D printing method is a suitable for the coating purposes.

Potential applications

Owing to their distinct advantages, optical fiber sensors have become the focus of extensive research and are now applied in various domains, such as healthcare, industrial regimes, and environmental monitoring. Efforts to improve the performance of these sensors often involve the functionalization of optical fibers with plasmonic materials. Au and Ag, in particular, are widely utilized plasmonic materials, and many investigations have explored the integration of Au/Ag NCs into optical fiber sensors. The potential applications for such sensors are summarized in **Table 3**.

Table 3 Applications of optical fiber sensor functionalized with Au/Ag-based structures.

No	Material	Optical Fiber Structure	Plasmonic Effect	Sensing Application	Ref.
1	Au/Ag	NCF	SPR	Salinity sensor	[11]
2	Au@AgPt NSs	MMF-SMF-MMF	LSPR	Copper ion (II) sensor	[13]
3	Au/Ag	MMF-NCF-MMF	SPR	Refractive index and temperature sensor	[32]
4	Au@Ag doped ternary matrix	MMF with beveled tip	SPR	Vitamin A sensor	[33]
5	Au core-Ag	-	LSPR	Monitoring cyanide levels in water	[34]
6	Ag/Au, Au/Ag bimetallic with LCC	TOF	SPR	Refractive index sensor	[35]
7	AuNPs-coated AgNPs	U-shaped	SPR	Biosensor for vitamin B1	[45]
8	Au/Ag	D-shaped MMF	SPR	Refractive index sensor	[46]
9	Au/Ag	FOSPR	SPR	Biosensor	[47]
10	Graphene-Gold-Au@Ag NPs-PDMS	MMF-SMF-MMF	SPR	Refractive index and temperature sensor	[86]
11	Ag/Au	MMF-NCF-MMF	SPR	Refractive index and pH sensors	[87]
12	Ag@Au nanorods	SMF	LSPR	Refractive index sensor	[88]
13	Au/Ag	SMF	SPR	Temperature sensor	[89]

No	Material	Optical Fiber Structure	Plasmonic Effect	Sensing Application	Ref.
14	Au/Ag	Y-shaped	SPR	Glucose and cortisol sensors	[90]
15	Au/Ag	Plastic-clad optical fiber	SPR	Glucose and cortisol sensors	[91]
16	Au/Ag@Au nanoparticles	Fiber SPR	SPR	Fluoroquinolone residues	[92]
17	Au/Ag spherical nanoparticles film	Uncladed optical fiber	SPR	SARS-CoV-2 detection	[93]
18	Au/Ag nanoparticles	Plastic optical fiber	LSPR	Optofluidic nanosensor	[94]
19	Core-shell Ag-Au	Photonic crystal fiber	SPR	Refractive index sensor	[95]
20	Au/Ag bimetallic nanorings	Thin cylindrical optical fiber	LSPR	Refractive index sensor	[96]
21	Ag-coated Au nanostars	Multimode fiber	LSPR	SERS detection	[97]

The combination of Au and Ag can elevate the optical fiber sensing performances. The functionalization of these materials trigger plasmonic effects. For example, previous research [46] applied a gold coating followed by silver, which effectively activated the SPR phenomenon on the optical fiber. Confinement loss occurs and plays a crucial role in the capability of the optical fiber sensor. This loss increases due to the SPR effect, enhancing the sensor's ability to detect analytes, including those at very low concentrations with high accuracy [46]. The study also suggested that the dimension of Au and Ag layers also influences the confinement loss, where the thicker the Au and Ag layers, the greater the confinement loss [46]. Furthermore, the sensing sensitivity is also influenced by the gap distance between the nanoparticles coated on the optical fiber. As in a previous report [13], when Au@AgPt NSs were immersed for too long on the optical fiber, the coated nanostructures became thicker and formed agglomerations which result in changes in the transmission spectrum and thus affect the sensitivity.

Applications of optical fiber sensors in the health sector such as in detecting vitamins A and B1 [33,45]. Au@Ag nanostructures incorporated into SiO_2-TiO_2-ZrO_2 ternary matrix could selectively detected vitamin A at concentrations between 10 and 1,000 μM [33]. Another study showed that an optical fiber sensor sequentially coated with AuNPs followed by an AgNPs layer was capable of sensing vitamin B1 within the detection range of 2 - 10 μM [45]. In addition, several previous researchers also stated that optical fiber sensors with Au-Ag coating were able to detect levels of cortisol, glucose (0 - 0.1 mM), and cholesterol (0 - 15 nM) [90,91]. SPR-based optical fiber using Au-Ag@Au NPs film was reported as effective device for the observing antibiotic residues in milk, meat, and aquatic products [92]. During the COVID-19 pandemic, which was announced by the World Health Organization (WHO) in March 2020 as the global pandemic and led to over 7 million deaths globally, researchers further explored the potential of this technology. Optical fiber sensors coated with Au/Ag nanoparticles film to detect SARS-CoV-2 virus [93]. Thus, the advance of optical fiber sensors has great potential in improving the quality of technology in the health sector.

The utilization of optical fiber sensors in industry such as in detecting copper ion (II) and cyanide has also been successfully carried out [13,34]. Cyanide is harmful to the body and is usually used in various industries such as Au and Ag mining. Au@Ag nanostructures coated optical fiber sensor could detect cyanide at the lowest concentration of 8×10^{11} M [13]. PEI-Au@AgPt nanostructures functionalized on optical fibers could measure Cu^{2+} ions at the lowest concentration 10^{-16} mol/L [34]. Optical fiber-based temperature sensors can be applied in the industrial world, where temperature is one of the important parameters in an industry [86]. In food industry sector, Ag-coated Au nanostars were coated on MMF for the SERS detection purpose [97]. In addition, temperature sensors can also be applied in the aerospace field, where aircraft engine temperatures need to be monitored to

prevent aircraft accidents. Based on previous research, optical fiber-based temperature sensors were able to detect temperatures with a range of 0 - 80 °C [32]. Furthermore, plastic optical fiber decorated with Au-Ag nanostructures for LSPR activation could be used for optofluidic nanosensor [94]. Therefore, optical fiber sensors have the potential to improve monitoring or sensing technology in the industrial world.

Measuring refractive indices is the fundamental application of Au/Ag NCs optical fibers, and therefore it has been widely investigated by many scientists [32,35,46,86-88,95,96]. The optical fiber sensor demonstrated a high sensitivity up to 3,309 nm/RIU for refractive index measurements [46].It relies on changes in the local refractive index near the optical fiber surface, which alter the optical properties of the nanocomposites and shift the resonance wavelength or transmitted light intensity. Such sensitivity makes these optical fibers valuable for further applications, for example in chemical detection [88], plasmoni sensing [96], and environmental monitoring [32,87]. Some environmental applications of optical fiber sensors included detection of pH [87], salinity [11], and temperature [32,89]. Recent advancements have led to the development of dual Au/Ag NCs-coated optical fiber sensors for simultaneously measuring multiple parameters. For instance, these sensors could detect both refractive index and pH changes [87], or concurrently monitor refractive index and temperature variations [32,89]. It implies that Au/Ag NCs-coated optical fiber sensors exhibit excellent versatility and practical utility in complex sensing environments.

Limitations and challenges

The advantages and potential applications of optical fiber sensors have attracted the attention of many experts. Nonetheless, they continue to face several limitations. Applications of optical fiber sensors involve various fiber structures tailored to specific uses. This indicates that the optical phenomena vary between different fiber structures. For example, the optical phenomenon that occurs in optical fibers with FBG structures is core mode coupling [98], while in NCF it is multi-modal interference (MMI) [55]. Thus, a more in-depth study is needed regarding the optical phenomena in optical fibers before being applied to certain optical fiber sensors. In addition, the small size and fragile nature of optical fibers [99], require modifications to enhance their mechanical strength for practical applications.

Plasmonic materials also play a critical role in elevating the performance of optical fiber sensors [97]. Materials with good optical properties are able to activate optical phenomena, such as SPR [32] and LSPR [34] in optical fiber sensors. Functionalization of plasmonic materials, especially Au/Ag NCs, on optical fibers has been widely used to trigger the SPR effect. However, in this field, LSPR using Au/Ag NCs is not as widely explored as SPR. Furthermore, the functionalization method used still mainly relied on SAM. Despite the promising optical responses of Au/Ag NCs, challenges remain in achieving uniform coatings with maintained stability [36].

Future research

Previous studies suggested that Au/Ag NCs coating could enhance the optical fiber sensing performance. Different synthesis methods have been carried out to obtain Au/Ag NCs with excellent characteristics. In addition to the nanomaterials, the structure of the optical fiber sensor itself significantly contributes to better performance. As a result, different fiber sensor configurations have been investigated to identify the most effective designs. Functionalization of Au/Ag NCs onto optical fiber sensors can be achieved through several techniques, with SAM being one of the most commonly employed methods due to their simplicity and effectiveness.

While optical fiber sensors have been increasingly applied in various fields, the number of applications involving sensors functionalized specifically with Au/Ag NCs remains relatively limited. Therefore, further studies are needed to develop optical fiber sensors functionalized with Au/Ag NCs across a broader range of applications, especially for simultaneous sensing purposes. Continued development of optical fiber structures is also essential to further maximize their potential. Additionally, alternative functionalization techniques beyond SAM are needed to improve adhesion, reproducibility, and long-term sensor performance. These actions will improve the potential of plasmonic nanocomposites in next-generation optical fiber sensors.

Conclusions

Au/Ag NCs have demonstrated the potential to improve the performance of optical fiber sensors. The characteristics of the synthesized Au/Ag NCs, which are influenced by the chosen synthesis method, play a crucial role in determining their effectiveness for coating in optical fiber sensors. The synthesis of Au/Ag NCs can be done by top-down or bottom-up approaches. Numerous optical fiber sensor designs have been engineered and optimized for specific applications, where both the structural configuration and nanomaterial coatings significantly influence sensing performances. To functionalize Au/Ag NCs onto optical fiber surfaces, several techniques have been employed, including self-assembly monolayer, electroless plating, and photochemical deposition. Different coating techniques provide specific advantages, including simplicity of the process, affordability, and the ability to precisely control coating parameters. Although optical fiber sensors functionalized with Au/Ag NCs have been developed in various fields, including healthcare, industry, and the environment, their implementation remains limited. Therefore, further research is crucial to broaden the scope of applications and to continue advancing the design and functionality of these promising sensing platforms.

Acknowledgements

This work is supported by the Matching Fund Research Grant, jointly funded by Universitas Negeri Malang and Universiti Teknologi Malaysia, awarded to N.H. and H.B. for the fiscal year 2025 under contract number 24.2.77/UN32.14.1/LT/2025.

Declaration of Generative AI in Scientific Writing

Generative artificial intelligence was not used for content creation or data analysis. The authors take full responsibility for the content and conclusions presented in this work.

CRediT Author Statement

Siti Azimatul Luthfiyyah: Methodology, Investigation, Writing – Original Draft, Writing – Review & Editing.

Sunaryono: Supervision, Validation, Writing – Review & Editing.

Hazri Bakhtiar: Resources, Funding Acquisition, Project Administration.

Arif Hidayat: Data Curation, Formal Analysis, Visualization.

Nurul Hidayat: Conceptualization, Supervision, Writing – Review & Editing, Funding Acquisition.

References

[1] A Prasanth, VK Harini, P Manivannan, S Narasimman, M Velumani, SR Meher and ZC Alex. A comparative study of ZnO, AZO, TiO_2, Sb_2O_3, and SnO_2 nanomaterials coated SPR based fiber optic refractive index sensors for chemical sensing application. *Optical Materials* 2024; **152**, 115438.

[2] F Tang, J Bai, G Li, Z Lin and HN Li. Monitoring under-coating corrosion of painted structural steel with no-core fiber optic sensors. *Measurement* 2024; **225**, 114075.

[3] T Han, C Zhang, H Yu and J Li. A disposable fiber-optic plasmonic sensor for chemical sensing. *Analytical Biochemistry* 2025; **696**, 115672.

[4] Y Feng, H Wu, MH Esmail, C Liu, X Liu, C Wang and T Shen. Research on lead ion sensing based on micro-nano fiber coupler cascade tilted fiber grating. *Optik* 2025; **322**, 172200.

[5] Y Wang, Z Liao, J Li and F Meng. ZnOHF-ZnO nanomaterial-coated macro-bend fiber triethylamine gas sensor working at room temperature. *Sensors and Actuators B: Chemical* 2024; **411**, 135733.

[6] X Ding, J Yan, N Chen, T Jin and R Zhang. Fiber-optic sensor modified by electrospun Polymer/Ti_3C_2 MXene-TiO_2 for dimethyl sulfoxide sensing. *Talanta* 2025; **287**, 127630.

[7] X Ding, J Yan, N Chen, T Jin and R Zhang. Highly sensitive balloon-like fiber interferometer based on GO nanomaterial coated for humidity measurement. *Optics & Laser Technology* 2023; **158**, 108798.

[8] M Song, X Jing, P Guo, Z Yin and S Li. SPR fiber optic sensor based on MMF-NCF doped with MgF_2 for dual-parameter measurement of temperature and humidity. *Optics Express* 2025; **33(2)**, 1869-1882.

[9] NTT Phuong, NHN Thao, HKT Ta, NQM Tran, TN Bach, BT Phan and NHT Tran. Application of hybrid Au@Ag nanostructures in fiber optic biosensor for rapid detection of C-reactive protein. *Optical Materials* 2023; **143**, 114184.

[10] J He, H Pan, L Feng and W Feng. Dual-channel fiber-optic biosensors based on LSPR and SPR for the trace detection of rabies virus. *Applied Physics Letters* 2025; **126(7)**, 073701.

[11] S Zhang, Y Zhao, Y Peng and JC Zhao. High-sensitivity optical fiber SPR sensor with cascaded biconical fiber and hetero-core structure for simultaneous measurement of seawater salinity and temperature. *Optics & Laser Technology* 2024; **170**, 110275.

[12] J Zhao, SM Deng, YN Zhang, F Xia, Y Zhao and HG Zhang. An *in situ* seawater salinity sensor with temperature self-compensation based on hollow-core fiber. *IEEE Transactions on Instrumentation and Measurement* 2025; **74**, 1-8.

[13] Q Huang, W Zhu, Y Wang, Z Deng, Z Li, J Peng, D Lyu, E Lewis and M Yang. Optical fiber plasmonic sensor for the ultrasensitive detection of copper (II) ion based on trimetallic Au@AgPt core-shell nanospheres. *Sensors and Actuators B: Chemical* 2020; **321**, 128480.

[14] B Glisic, D Inaudi, JM Lau and CC Fong. Ten-year monitoring of high-rise building columns using long-gauge fiber optic sensor. *Smart Materials and Structures* 2013; **22(5)**, 055030.

[15] K Yüksel, OD Merdin, D Kinet, M Merdin, C Guyot and C Caucheteur. FBG-based temperature and fire sensors for use in industrial microwave ovens. *In*: Proceedings of the 29th International Conference on Optical Fiber Sensors, Porto, Portugal. 2025, p. 1437-1440.

[16] Q Yu, Y Zhang, L Jiang, L Li, X Li and J Zhao. Flexible optical fiber sensor for non-invasive continuous monitoring of human physiological signals. *Small Methods* 2025; **9**, 2401368.

[17] X Zhou, S Wang, L Yu, Y Yang and L Gao. Scheme and algorithm designs for optical fiber sensors based configuration inversion of umbilical cables in deep-water. *Ocean Engineering* 2025; **332**, 12 1363.

[18] MS Soares, R Singh, S Kumar, R Jha, J Nedoma, R Martinek and C Marques. The role of smart optical biosensors and devices on predictive analytics for the future of aquaculture systems. *Optics & Laser Technology* 2024; **177**, 111049.

[19] I Petermann, M Lindblom, C Sterner, G Gregard and S Karlsson. Optical fiber sensor solutions for in-situ transmittance control of electrochromic glazing. *Advanced Sensor and Energy Materials* 2025; **4**, 100134.

[20] J Kozman and W Warsi. *Applied workflows for fiber optic sensing data from low carbon energy projects. In*: W Hu and BW Horn (Eds.). Fourth international meeting for applied geoscience & energy. Society of Exploration Geophysicists, Houston, Texas, USA, 2024, p. 607-611.

[21] Z Liu, Y Lu, X Ma, Y He, M Fu, S Yan, C Li, X Song, H Zhou and K Liu. Advanced functional optical fiber sensors for smart battery monitoring. *Energy Material Advances* 2024; **5**, 0142.

[22] Z Huang, C Mao, S Guan, H Tang, G Chen and Z Liu. Security threshold setting algorithm of distributed optical fiber monitoring and sensing system based on big data in smart city. *Soft Computing* 2023; **27(8)**, 5147-5157.

[23] S Wu, H Zheng, S Li, Y Wang and R Tong. An SPR-MZ interference-based fiber optic sensor for dual-parameter measurement of seawater temperature and salinity. *IEEE Sensors Journal* 2025. https://doi.org/10.1109/JSEN.2025.3571761

[24] E Ling Wei Hong, SS Chong and FF Chung. Quasi-distributed polymer fiber optics sensor based on wavelength-intensity-coupled dual-measurement for multiplex localization sensing, *Sensor Review* 2025. https://doi.org/10.1108/SR-12-2024-0985

[25] M Irigoyen, JA Sánchez-Martin, E Bernabeu and A Zamora. Tapered optical fiber sensor for chemical pollutants detection in seawater. *Measurement Science and Technology* 2017; **28(4)**, 045802.

[26] X Kong, M Li, W Xiao, Y Li, Z Luo, JW Shen and Y Duan. Ω-shaped fiber optic LSPR coated with hybridized nanolayers for tumor cell sensing and photothermal treatment. *Talanta* 2024; **278**, 126381.

[27] SR Makhsin, MH Zakaria, MH Noor Akashah, R Abdul Rani, PJ Scully and P Gardner. Enhancing

fibre optic sensor signals via gold nanoparticle-decorated agarose hydrogels. *Optical Materials* 2023; **143**, 114247.

[28] JD Lopez-Vargas, A Dante, RC Allil, I Del Villar, IR Matias and MM Werneck. Ag@Fe_3O_4-coated U-shaped plastic optical fiber sensor for H_2S detection. *Sensors and Actuators B: Chemical* 2024; **401**, 135054.

[29] M Alhajj, M Aziz, H Bakhtiar, N Hidayat, M Safwan and SK Ghoshal. Enhanced fluorescence response and effective petroleum sensing performance of silver/copper nanocomposites. *Materials Chemistry and Physics* 2025; **333**, 130342.

[30] S Islam and A Alshoaibi. Crack-alleviated gold-assisted silica-titania 3-layered fiber optic pH sensor. *Materials Chemistry and Physics* 2024; **316**, 129102.

[31] NS Najah, LA Nabila, R Rusidah, SA Luthfiyyah, A Taufiq and N Hidayat. Pulsed Nd:YAG laser-synthesized silver nanoparticles with high sensitivity for glucose detection. *Suranaree Journal of Science and Technology* 2025; **32**, 030311.

[32] Z Yin, K Li, X Jing, S Ullah and Z Zhang. A broadband SPR sensor based on a no-core fiber coated with gold-silver for refractive index and temperature measurement. *Infrared Physics & Technology* 2023; **132**, 104756.

[33] VP Prakashan, G Gejo, MS Sanu, MS Sajna, T Subin, PR Biju, J Cyriac and NV Unnikrishnan. Sensor serat optik berbasis SPR baru untuk vitamin A menggunakan nanopartikel cangkang inti Au@Ag yang didoping matriks terner SiO_2-TiO_2-ZrO_2 (*in Indonesian*). *Applied Surface Science* 2019; **484**, 219-227.

[34] NTT Phuong, VD Phung, TBN Le, T Chi, BTT Hien, LH Tho, NXD Mai, TB Phan, NHT Tran and H Ju. Ultrasensitive monitoring of cyanide concentrations in water using a Au_{core}-Ag_{shell} hybrid-coating-based fiber optical sensor. *Langmuir* 2023; **39(44)**, 15799-15807.

[35] J Korec, KA Stasiewicz and LR Jaroszewicz. SPR sensor based on a tapered optical fiber with a low refractive index liquid crystal cladding and bimetallic Ag-Au layers. *Sensors* 2022; **22(19)**, 7192.

[36] N Hidayat, MS Abd Aziz, H Nur, A Taufiq, N Mufti, RR Mukti and H Bakhtiar. Sensitivity enhancement of gold nanospheres assisted CO_2 laser tapered optical fiber for refractive index sensor. *Optical Fiber Technology* 2023; **77** 103275.

[37] J Feng, J Gao, W Yang, R Liu, M Shafi, Z Zha, C Liu, S Xu, T Ning and S Jiang. LSPR optical fiber sensor based on 3D gold nanoparticles with monolayer graphene as a spacer. *Optics Express* 2022; **30(6)**, 10187-10198.

[38] B Karki, A Jha, A Pal and V Srivastava. Sensitivity enhancement of refractive index-based surface plasmon resonance sensor for glucose detection. *Optical and Quantum Electronics* 2022; **54(9)**, 595.

[39] RA Mahmud, RH Sagor and MZM Khan. Surface plasmon refractive index biosensors: A review of optical fiber, multilayer 2D material and gratings, and MIM configurations. *Optics & Laser Technology* 2023; **159**, 108939.

[40] Y Zhang, Y Sun, L Cai, Y Gao and Y Cai. Optical fiber sensors for measurement of heavy metal ion concentration: A review. *Measurement* 2020; **158**, 107742.

[41] YS Alqahtani, AM Mahmoud, M Khateeb, R Ali and MM El-Wekil. Near-infrared fluorescent probe for selective and sensitive detection of glutathione based on thioctic acid-functionalized Ag/Au NCs-assisted by ferric ion. *Microchemical Journal* 2024; **201**, 110752.

[42] Y Su, P Gao, G Zhang, Y Zhou, L Shi, J Wu, W Liang, S Shuang and Y Zhang. Multifunctional Au–Ag NCs for luminescence and colorimetric double signal sensing of H2S and catalytic reduction of nitrophenol. *Talanta* 2025; **282**, 127022.

[43] X Liu, Y Zhang, X Cai, D Yang and Y Zhu. Atomically modified Au-/Ag-based nanoclusters towards enhanced photoluminescence. *CCS Chemistry* 2024; **7(3)**, 620-636.

[44] Y Gao, X He, R Hu and Q Li. Dual quenching mechanism study and application for sensitive sensing acid phosphatase activity based on bimetallic Au/Ag nanoclusters with enhanced fluorescence. *Microchemical Journal* 2024; **204**, 111077.

[45] A Li, X Wen, H Ma, X Yang, H Jiang, P Teng, B Zhang, K Li, S Sivanathan and MA Roula. Smartphone-based selective and sensitive detection of vitamin B1 in synthetic urine using U-bend SPR optical fiber probe. *Optical Fiber Technology* 2024; **84**, 103769.

[46] MR Thayalan, MF Azman, SMA Musa, Z Yusoff and SA Ibrahim. Surface plasmon resonance in gold-silver bilayer coated D-shaped multimode optical fiber: An approach to refractive index sensing. *Results in Optics* 2024; **16**, 100680.

[47] M Lu, Y Liang, S Qian, L Li, Z Jing, JF Masson and W Peng. Optimization of surface plasmon resonance biosensor with Ag/Au multilayer structure and fiber-optic miniaturization. *Plasmonics* 2017; **12**, 663-673.

[48] FD Algahtani, MT Elabbasy, AH Asghar, NE Elhassan, S Gdaim, MA El-Morsy, MO Farea and AA Menazea, Tunning Silver@Gold core@shell incorporated in poly (vinyl alcohol) via laser ablation: Antibacterial activity and cell viability behavior for wound healing. *Journal of Saudi Chemical Society* 2023; **27(3)**, 101637.

[49] N Bi, Y Zhang, Y Xi, M Hu, W Song, J Xu and L Jia. Colorimetric response of lysine-caped gold/silver alloy nanocomposites for mercury(II) ion detection. *Colloids and Surfaces B: Biointerfaces* 2021; **205**, 111846.

[50] G Lanza, D Betancourth, A Avila and H Riascos. Control of the size distribution of AuNPs for colorimetric sensing by pulsed laser ablation in liquids. *Kuwait Journal of Science* 2025; **52(1)**, 100294.

[51] NM Mwenze, M Juma, M Maaza, Z Birech and MS Dhlamini. Laser liquid ablation for silver nanoparticles synthesis and conjugation with hydroxychloroquine for Covid-19 treatment. *Materials Today: Proceedings* 2023. https://doi.org/10.1016/j.matpr.2023.08.195.

[52] Z Qiu, X Liu, Y Zhang, S Zhu, M Chen, Y Zhao and X Luo. Enzymatic ablation of bimetallic Au@Ag nanocomposites enabling the smartphone-based colorimetric visualization of S1 nuclease. *Sensors and Actuators B: Chemical* 2025; **432**, 137487.

[53] X Zeng, H Chen, F Long, X She, W Lan, W Long, S Wang, L Wei, Y She and H Fu. Cloud machine learning-enhanced peroxidase-like enzyme visual sensor for rapid detection of sulfur-containing pesticides. *Sensors and Actuators B: Chemical* 2025; **431**, 137448.

[54] Y Ren, W Yang, Z Tan, L Zhang and R Pan. A high-sensitivity balloon-type optical fiber sensor enables wide-range strain sensing with the assistance of CNN. *Measurement* 2024; **237**, 115254.

[55] Y Li, X Li, Y Liu, J You, Y Peng and H Chen. High sensitivity Mach-Zehnder interferometric fiber-optic humidity sensor based on multimode interference enhancement. *Optical Fiber Technology* 2024; **87**, 103891.

[56] Y Wang, C Shen, W Lou and F Shentu. Fiber optic humidity sensor based on the graphene oxide/PVA composite film. *Optics Communications* 2016; **372**, 229-234.

[57] Y Wang, C Shen, W Lou, F Shentu, C Zhong, X Dong and L Tong. Fiber optic relative humidity sensor based on the tilted fiber Bragg grating coated with graphene oxide. *Applied Physics Letters* 2016; **109(3)**, 031107.

[58] S Lin, F Wang, Y Qu, X Han and Y Zhang. Discharge splicing-free ultra-highly sensitive fiber-optic temperature sensor based on PDMS and the Vernier effect. *Sensors and Actuators A: Physical* 2024; **376**, 115653.

[59] F Chen, S Sheng, W Jiang, Z Tu, Q Jiang, M Huang, C Jiang, J Wen and S Sun. Ultra-sensitive fiber-optic temperature sensor based on UV glue-based FPI and Vernier effect. *Infrared Physics & Technology* 2024; **139**, 105311.

[60] H Su, Y Wang, C Guan, S Yu, X Yu and W Yang. PDMS-sensitized MZI fiber optic temperature sensor based on TCF-NCF-TCF structure. *Optical Fiber Technology* 2022; **73**, 103075.

[61] Y Liu, Y Zhang, S Liu, B Shi, L Wang and Y Zhao. Fiber optic room temperature ethanol sensor based on $ZnSnO_3/TiO_2$ with UV radiation sensitization. *Sensors and Actuators B: Chemical* 2024; **399**, 134814.

[62] V Handerek. *Single mode optical fiber sensors. In*: KTV Grattan and BT Meggitt (Eds.). Optical fiber sensor technology. Springer, Dordrecht, Netherlands, 1995, p. 197-222.

[63] Y Koike and K Koike. *Optical fibers. In*: K Matyjaszewski and M Möller (Eds.). Polymer science: A comprehensive reference. Elsevier, Amsterdam, Netherland, 2012, p. 283-304.

[64] R Hui. *Optical fibers. In*: R Hui (Ed.). Introduction to fiber-optic communications. Elsevier, Amsterdam, Netherland, 2020, p. 19-76.

[65] R Ramaswami, KN Sivarajan and GH Sasaki. *Propagation of signals in optical fiber. In*: R Ramaswami, KN Sivarajan and GH Sasaki (Eds.). Optical networks. Elsevier, Amsterdam, Netherland, 2010, p. 47-112.

[66] SV Ahamed. *Optical fiber in modern networks. In*: SV Ahamed (Ed.). Intelligent networks. Elsevier, Amsterdam, Netherland, 2013, p. 93-106.

[67] NM Razali, MQ Lokman, SNF Zuikafly, F Ahmad, MA Abdul Rahman, H Yahaya and SW Harun. No-core fiber by self-image length optimization for optical based refractive index sensor. *Optical Fiber Technology* 2022; **74**, 103133.

[68] Z Xie, Z Huang, Y Shi, Y Cao, J Dong, R Tian and C Shen. Highly sensitive optical fiber hydrogen detection in liquid environment. *International Journal of Hydrogen Energy* 2025; 106, 1-7.

[69] J Xi, H Sun, J Li, L Deng, Y Yang, H Zheng, D Feng, X Huang, J Zhang and X Li. Tilted fiber Bragg grating sensor based on surface plasmon resonance and electrospinning for glucose detection. *Microchemical Journal* 2024; **204**, 110978.

[70] W Udos, CW Ooi, KS Lim, N Yusof, ML Low, R Zakaria, WR Wong and H Ahmad. Surface plasmon sensor for lead ion (Pb^{2+}) detection using graphene oxide - Gold coated tilted fiber Bragg grating. *Results in Optics* 2023; **12**, 100502.

[71] X Liu, R Singh, B Zhang, C Caucheteur, N Santos, S Kumar, J Nedoma and C Marques. Advanced fiber optic sensors for quantitative nitrite detection: Comparative analysis of plasmonic tilted fiber Bragg gratings and fiber optic tips with ion-imprinted polymers. *Sensors and Actuators Reports* 2024; **8**, 100233.

[72] S Mishra, P Sharan, AN Alodhayb, TA Alrebdi and AM Upadhyaya. Design and development of wagon load monitoring system using fibre Bragg grating sensor. *Optical Fiber Technology* 2025; **90**, 104149.

[73] J Zhang, X Shen, M Qian, Z Xiang and X Hu. An optical fiber sensor based on polyimide coated fiber Bragg grating for measurement of relative humidity. *Optical Fiber Technology* 2021; **61**, 102406.

[74] B Wang, L Cai and Y Zhao. An optical fiber sensor for the simultaneous measurement of pressure and position based on a pair of fiber Bragg gratings. *Optical Fiber Technology* 2021; **67**, 102742.

[75] M Lydon, D Robinson, SE Taylor, G Amato, EJO Brien and N Uddin. Improved axle detection for bridge weigh-in-motion systems using fiber optic sensors. *Journal of Civil Structural Health Monitoring* 2017; **7**, 325-332.

[76] Z Samavati, A Samavati, AF Ismail, MA Rahman, MHD Othman and FN Yeganeh. Optical fiber sensor for glycoprotein detection based on localized surface plasmon resonance of discontinuous Ag-deposited nanostructure. *Optical Fiber Technology* 2021; **62**, 102476.

[77] T Liu, X Xiao and C Yang. Surfactantless photochemical deposition of gold nanoparticles on an optical fiber core for surface-enhanced Raman scattering. *Langmuir* 2011; **27(8)**, 4623-4626.

[78] HM Kim, HJ Kim, SC Yang, JH Park and SK Lee. Fiber optic localized surface plasmon resonance hydrogen sensor based on gold nanoparticles capped with palladium. *Journal of Industrial and Engineering Chemistry* 2022; **111**, 281-288.

[79] K Sadani, P Nag and S Mukherji. LSPR based optical fiber sensor with chitosan capped gold nanoparticles on BSA for trace detection of Hg (II) in water, soil and food samples. *Biosensors and Bioelectronics* 2019; **134**, 90-96.

[80] M Loyez, C Ribaut, C Caucheteur and R Wattiez. Functionalized gold electroless-plated optical fiber gratings for reliable surface biosensing. *Sensors and Actuators B: Chemical* 2019; **280**, 54-61.

[81] Y Huang, X Pu, H Qian, CJ Chuang, S Dong, J Wu, J Xue, W Cheng, S Ding and S Li. Optical fiber surface plasmon resonance sensor using electroless-plated gold film for thrombin

detection. *Analytical and Bioanalytical Chemistry* 2024; **416(6)**, 1469-1483.

[82] X Zheng, D Guo, Y Shao, S Jia, S Xu, B Zhao, W Xu, C Corredor and JR Lombardi. Photochemical modification of an optical fiber tip with a silver nanoparticle film: A SERS chemical sensor. *Langmuir* 2008; **24(8)**, 4394-4398.

[83] T Liu, W Wang, F Liu and S Wang. Photochemical deposition fabricated highly sensitive localized surface plasmon resonance based optical fiber sensor. *Optics Communications* 2018; **427**, 301-305.

[84] D Chekkaramkodi, I Ahmed, RKA Al-Rub, A Schiffer and H Butt. 3D-printed multi-material optical fiber sensor for dual sensing applications. *Advanced Composites and Hybrid Materials* 2025; **8(1)**, 107.

[85] F Alam, M Elsherif, AE Salih and H Butt. 3D printed polymer composite optical fiber for sensing applications. *Additive Manufacturing* 2022; **58**, 102996.

[86] Q Huang, Y Wang, W Zhu, T Lai, J Peng, D Lyu, D Guo, Y Yuan, E Lewis and M Yang. Graphene-gold-Au@Ag NPs-PDMS films coated fiber optic for refractive index and temperature sensing. *IEEE Photonics Technology Letters* 2019; **31**, 1205-1208.

[87] L Hu, J Li, Z Yin, Z Zhang, H Li, S Li, P Wang, H Du and R Wang. A cascade SPR sensor based on Ag/Au coated coreless optical fiber for RI and pH measurement. *Optics & Laser Technology* 2025; **180**, 111452.

[88] PSS dos Santos, JP Mendes, I Pastoriza-Santos, JP Juste, JMMM de Almeida and LCC Coelho. Gold-coated silver nanorods on side-polished singlemode optical fibers for remote sensing at optical telecommunication wavelengths. *Sensors and Actuators B: Chemical* 2025; **425**, 136936.

[89] M Xiong, C Teng, M Chen, Y Cheng, S Deng, F Li, H Deng, H Liu and L Yuan. Simulation study of high sensitivity fiber SPR temperature sensor with liquid filling. *Sensors* 2022; **22**, 5713.

[90] X Wang, X Sun, Y Hu, L Zeng and J Duan. Plasmonic dual-parameter optical fiber sensor for cortisol and glucose detection. *Optik* 2023; **284**, 170933.

[91] X Wang, X Sun, Y Hu, L Zhang, L Zeng, Q Liu and J Duan. A dual-parameter optical fiber SPR sensor for simultaneous measurement of glucose and cholesterol concentrations. *IEEE Sensors Journal* 2022; **22(21)**, 20413-20420.

[92] Q Xu, H Yin, Z Zhao, M Cui, R Huang and R Su. An Au-Ag@Au fiber surface plasmon resonance sensor for highly sensitive detection of fluoroquinolone residues. *Analyst* 2025; **150**, 877-886.

[93] Y Saad, MH Gazzah, K Mougin, M Selmi and H Belmabrouk. Sensitive detection of SARS-CoV-2 using a novel plasmonic fiber optic biosensor design. *Plasmonics* 2022; **17(4)**, 1489-1500.

[94] RPN dos Santos, LV Costa, FA e Silva, DB de Moraes, RCSB Allil, TS Rodrigues, MM Werneck and TA Balbino. Refractive index-sensitive optofluidic nanosensor using plastic optical fiber decorated with mono/bimetallic plasmonic nanoparticles. *Optics & Laser Technology* 2025; **183**, 112309.

[95] B Liu, Y Lu, X Yang and J Yao. Surface plasmon resonance sensor based on photonic crystal fiber filled with core-shell Ag-Au nanocomposite materials. *Optical Engineering* 2016; **55(11)**, 117104.

[96] S Shi, A Li, R Huang, J Yu, S Li, W Qi, Z He and R Su. *In situ* growth of Au-Ag bimetallic nanorings on optical fibers for enhanced plasmonic sensing. *Journal of Materials Chemistry C* 2020; **8(22)**, 7552-7560.

[97] Y Ran, P Strobbia, V Cupil-Garcia and T Vo-Dinh. Fiber-optrode SERS probes using plasmonic silver-coated gold nanostars. *Sensors and Actuators B: Chemical* 2019; **287**, 95-101.

[98] X Zhong, Q Xie, Y Liu, Y He, N Zhong, Z Zhang, H Karimi-Maleh, X Peng and E Lichtfouse. Recent advances in optical fiber grating sensors for detection of organic substances. *Chemical Engineering Journal* 2024; **492**, 152260.

[99] K Anjana, M Herath and J Epaarachchi. Optical fibre sensors for geohazard monitoring - A review. *Measurement* 2024; **235**, 114846.